Transactions of the SMiRT 27
Yokohama, Japan, March 3-8, 2024
Division V

COMPUTATIONAL SIMULATION OF LOW-RISE REINFORCED CONCRETE SHEAR WALLS SUBJECT TO ASR AND REVERSED CYCLIC LATERAL LOADING

Huan Li[1], Jose Pires[2]

[1] Structural Engineer, Division of Engineering, Office of Nuclear Regulatory Research, U.S. Nuclear Regulatory Commission, Mail Stop O5G10, Washington D.C., 20555-0001 (huan.li@nrc.gov).
[2] Sr. Technical Advisor, Division of Engineering, Office of Nuclear Regulatory Research, US Nuclear Regulatory Commission, Mail Stop O5G10, Washington D.C., 20555-0001 (jose.pires@nrc.gov).

ABASTRACT

This paper compares results of computational simulations to the test results conducted by the University of Toronto and sponsored by the Canadian Nuclear Safety Commission (CNSC). The seismic behaviour of non-ASR-affected shear walls, called regular shear walls (REG A and REG B), and ASR-affected concrete shear walls (ASR A1, ASR B1 and ASR B2) were tested and simulated. The load capacity, ductility, and energy dissipation for the shear walls with regular concrete remained similar for up to 995 days after casting; however, some differences were observed in the failure modes of these walls. The shear walls with ASR concrete tested at about 6 months after casting had ductility comparable to that of the regular walls but somewhat higher energy dissipation capacity and peak strength. The shear walls with ASR tested at about 1.5 years and 3 years had less ductility and energy dissipation capacity than the regular shear walls and the shear wall with ASR tested at 6 months but had similar peak strength.

3D finite element analyses presented here captured relatively well the peak load capacity and ductility of the regular walls and the walls with ASR tested at about 6 months after casting. The analyses also matched the peak capacity of the shear walls tested at 1.5 and 3 years after casting but did not capture the decrease in ductility and energy dissipation observed in the tests. A limited parametric study was conducted to assess modelling or input conditions, namely free-field ASR expansion, aggregate size, which would capture the decrease in ductility and energy dissipation for the walls with ASR tested for this benchmark study.

INTRODUCTION

Alkali silica reaction (ASR) has been observed in one nuclear power plant (NPP) in the United States and one NPP in Canada. ASR is a consequence of the presence of certain types of siliceous minerals in the concrete aggregates. Chemical expansion from ASR causes internal deterioration of the concrete material, which affects its mechanical properties and, under certain circumstances, may affect its structural performance or behaviour. Understanding the correlations between ASR concrete damage and structural behaviour is of interest when considering extended periods of operation for NPPs.

The Working Group in the Integrity and Aging of Components and Structures (IAGE) of the Committee on the Safety of Nuclear Installations (CSNI) of the Nuclear Energy Agency (NEA) initiated a cooperative research activity to assess effects of concrete pathologies on concrete structures in nuclear installations called Assessment of Structures Subjected to Concrete Pathologies called ASCET. The Canadian Nuclear Safety Commission (CNSC) initiated and funded a research program at the University of Toronto to study ASR concrete degradation mechanisms and to correlate ASR degradation to mechanical and structural behavior.

The scope of the work described here includes performing a limited parametric analysis of the tested walls used in conjunction with the available test data. The analyses presented used 3D finite element models of the tested walls using the reinforced concrete models, including the modelling of ASR degradation effects. The VecTor3 software developed by the University of Toronto (Wong, Vecchio and Trommels, 2002) was used for the analyses.

The following presents a summary of the shear wall tests and data available to the round-robin analyses, the model used for the analysis, the input data for the modelling, and results of the limited parametric analyses.

SHEAR WALL TESTS

In this section, the shear wall tests conducted at the University of Toronto are briefly summarized so that the simulation results provided in the following section can be compared with the test results.

As the structural part of the research program funded by the CNSC, the steel-reinforced shear walls made with ASR concrete and concrete were tested. As a part of Phase 1, Phase 2, and Phase 3 of research program, five shear walls were constructed, two regular walls (REG A, REG B) and three ASR walls (ASR A1, ASR B1, ASR B2) along with their control specimens. All the shear walls and the control specimens such as cylinders and prisms were conditioned in a special chamber with a high temperature of 50°C and 95% high humidity to accelerate the reaction and deterioration.

The shear wall was laterally constrained on both ends of the bottom concrete beam to prevent any slippage, and the shear wall specimens were also anchored to the strong floor to constrain vertical movement. In addition, a constant axial load of 800 KN was applied and maintained throughout the test on the top surface of the top concrete beam.

Test Setup

The test setup (Figure 1(a)) and the applied reversed cyclic displacement as well as the locations of LVDTs are shown in Figure 1 below (Habibi et al., 2015).

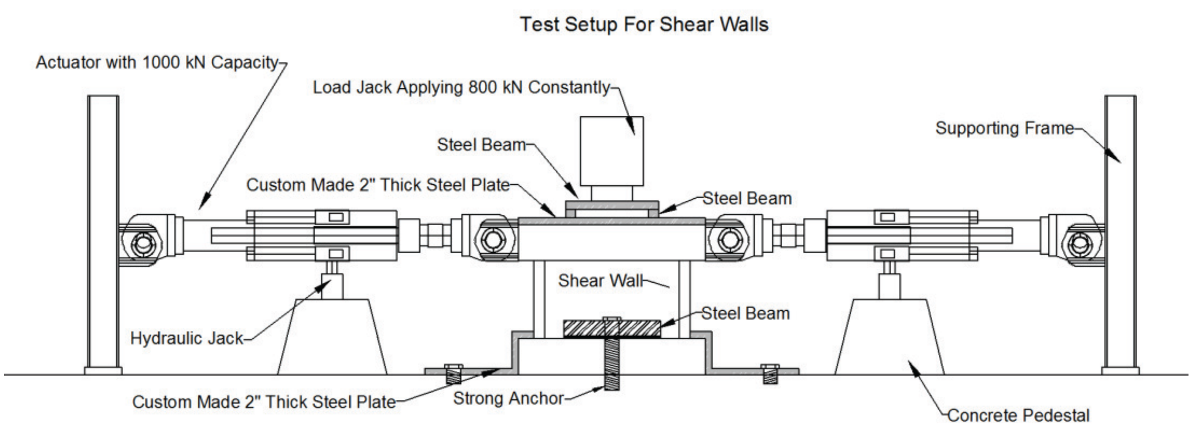

(a)

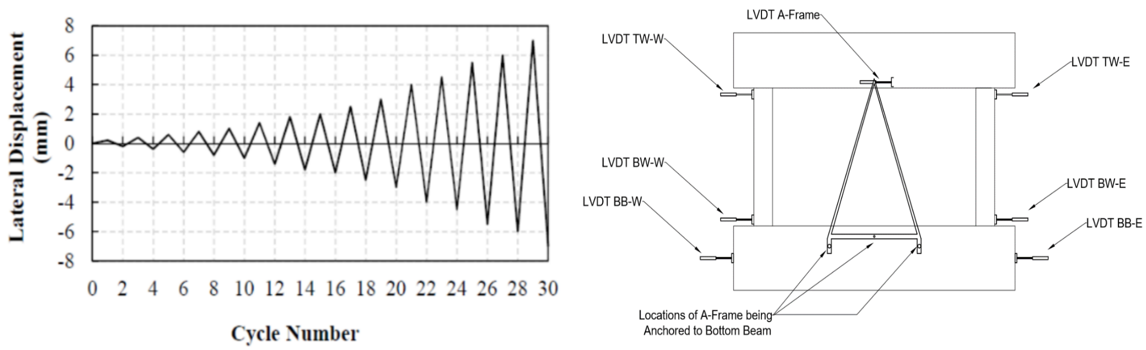

(b) (c)

Figure 1. (a) Testing setup (b) applied reversed cyclic displacement and (c) Location of LVDTs

To simulate seismic loads, lateral reversed displacement (Figure 1(b)) was applied by using two 1,000 KN actuators one on each side of the top concrete beam (Figure 1(a)). Seven LVDTs were used to measure the horizontal displacement along the height of the specimen from bottom beam to the top beam on both sides of the specimen (Figure 1(c)).

Test Results

The tests of the regular concrete shear walls and ASR-affected shear walls were conducted at an age from 240 days and 995 days. Figures 2 and 3 show the load-deflection curves from the test for both regular walls and ASR-affected concrete walls, respectively.

As shown in Figure 2, for the two regular shear walls, the only differences are their age and duration for which these walls were cured. REG A was tested after 220 days of curing in the environmental chamber while REG B was tested after 975 days of curing. Both walls show a very similar hysteretic response.

Comparing the hysteretic responses of three ASR walls, it is shown in Figure 3 that the ultimate shear capacity of the ASR shear walls were very similar, but the displacement at failure were different, which was decreased from 7.1 mm to 2.6 mm as the duration for the curing increased from 260 days to 995 days, as summarized in Table 1.The ductility of the shear walls is evaluated by comparing the strain energy calculated as the sum of areas enclosed under the force-displacement loops for each shear wall (see Table 1). It is shown that the strain energy of ASR wall decreases as the duration for the curing increases.

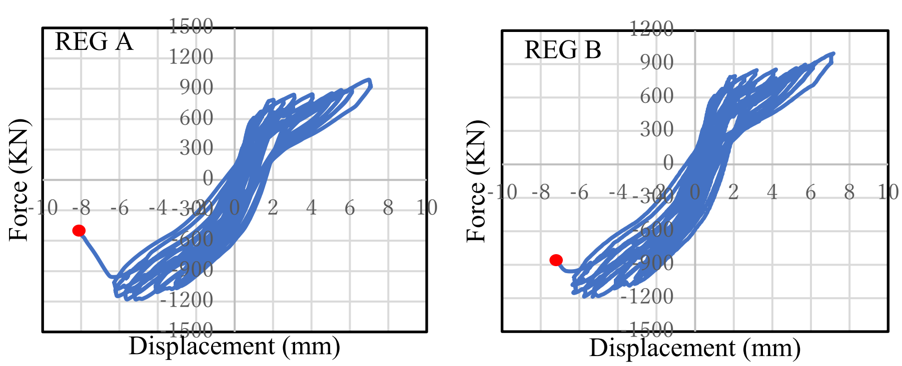

Figure 2. Lateral Load vs. Deflection Curves from the Test for Regular Concrete Shear Wall

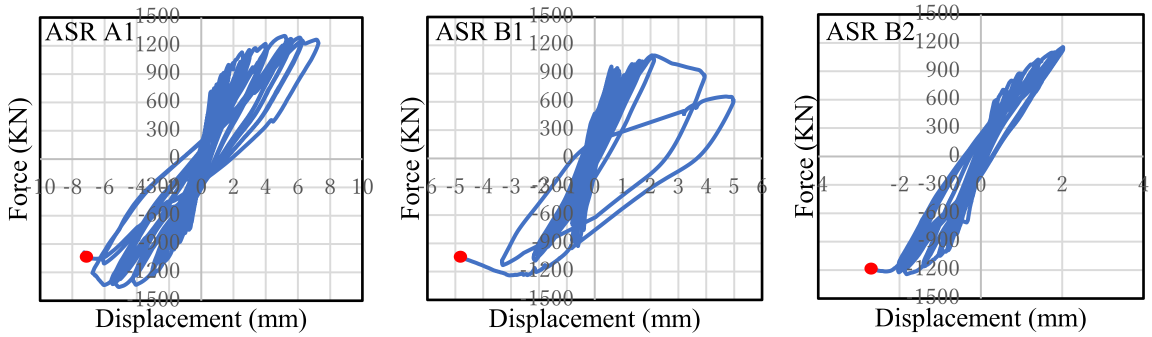

Figure 3. Lateral Load vs. Deflection Curves from the Test for ASR Concrete Shear Walls

Table 1. The Tested Shear Wall Peak Shear Capacities and Displacement

Wall	Age (days)	Peak Force (KN)	Maximum Displacement at Failure (mm)	Strain energy (J)
REG A	240	1180	8.2	31081
REG B	975	1187	7.3	28759
ASR A1	260	1355	7.1	37766
ASR B1	610	1240	4.9	17278
ASR B2	995	1243	2.6	7183

Note: The maximum displacements at failure are indicated by solid red circles in Figures 2 and 3.

The ASR walls show a bit higher peak shear capacities than the regular walls. Although the reasons for higher shear capacity for the ASR-affected wall than for the regular concrete wall are unclear, a possible explanation is that the ASR expansion would stress the reinforcing steel in tension, which would then confine the concrete. This confinement would then enhance the performance of the ASR shear walls. Boundary conditions also provide additional concrete confinement under the ASR expansion.

Since all the shear walls have identical vertical reinforcement ratios in both the panel section and boundary elements, similar peak shear strengths were observed for ASR walls. In addition, boundary elements with confining reinforcement in low aspect shear walls help maintain peak shear strength at cycles of displacement beyond peak strength. In general, similar shear strength is observed in all walls which was maintained for cycles of displacement beyond those at peak strength. However, for the walls tested 610 to 995 days after casting and with higher ASR expansions, failure in the tests was more sudden than for the wall with regular concrete and the wall with ASR tested at 260 days which implies less ductility.

FINITE ELEMENT ANALYSIS

Modelling Approach

All finite element analyses for this study used 3D nonlinear finite element analysis modelling and the VecTor3 software for the structural analysis of reinforced concrete components developed by Professor F. Vecchio and his research associates at the University of Toronto.

The theoretical bases for the modelling of the shear behaviour of reinforced concrete in VecTor3 are the Modified Compression Field Theory (Vecchio and Collins, 1986) and the Disturbed Stress Field Model

(Vecchio, 2000) used in conjunction with conceptual models for reinforced concrete based on a smeared rotating-crack macro-modelling approach. The researchers at the University of Toronto implemented ASR constitutive models within the architecture of VecTor3. These models treat the ASR expansion as non-recoverable offset strains using a computational procedure previously developed for elastic and plastic offset strains (Vecchio, 1992 and Jurcut, 2015). In addition, to consider the effects of ASR, the analysis also needs to take into account the expected unconfined material expansion and changes in mechanical properties.

Modeling Assumptions

The 3D finite element analysis model is shown in Figure 4. The thickness of top and bottom concrete blocks is 550mm, and 200mm for the wall flanges and 100mm for the web in thickness. Figure 4 shows the concrete and reinforcement configurations for the walls whose dimensions are listed in Table 2. The reinforcement was modelled in two ways, i.e., smeared reinforcement and discrete reinforcement. The total number of solid elements is 13296, and the total number of truss elements for the models with discrete reinforcement modelling is 1120. Spacing for the 10M rebar (100mm^2) is 140mm in both the vertical direction and the horizontal direction. Vertical spacing for the 6mm diameter stirrups in the flanges is 100mm.

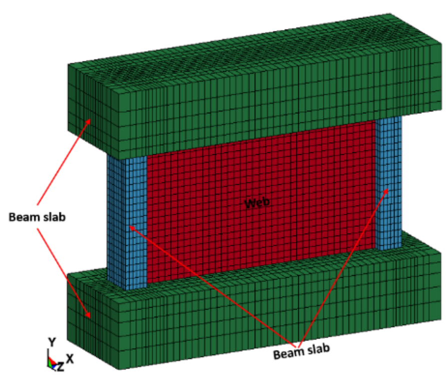

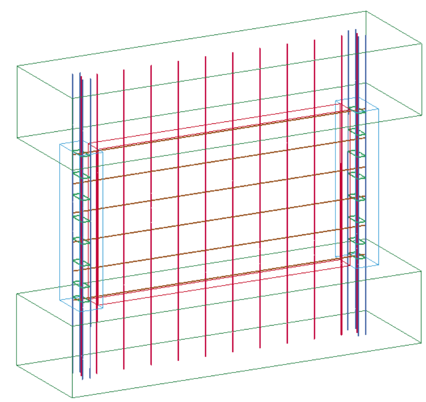

Figure 4. Shear wall concrete configuration (left) and reinforcement configuration (right)

Table 2. Concrete Dimensions

Component	**X**	**Y**	**Z**
Beam slab (mm)	1800	345	550
Flange (mm)	120	750	200
Web (mm)	1300	750	100

Boundary and Loading Conditions

As shown in Figure 5, the analysis fixed the vertical displacements at the bottom of the support block and the horizontal displacement at the center of gravity (CG) of the bottom support block. Gravity loads were applied to the entire model, and vertical nodal forces were applied at the upper surface of the top block to account for a total vertical force of 800 KN. The analysis then applied the reversed cyclic horizontal displacements (shear loading) shown in Figure 5 at the CG of the top block. One additional initial step of the analysis was the application of the ASR expansion and the calculation of the resulting strains and stresses in the concrete and reinforcement prior to the application of the vertical load and shear loading.

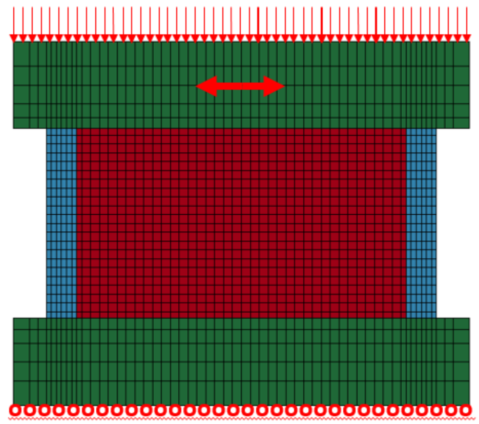

Figure 5. Boundary and Loading Conditions

Material Properties

Tables 3 to 6 summarize the material properties for the concrete and reinforcement, the reinforcement ratios as well as test results of ASR expansion for the shear wall components (Habibi et al., 2015).

Table 3. Concrete Properties from the Tests

Specimen	Age (days)	f'_c (MPa)	E_c (MPa)	f_t (MPa)
Regular A	240	79.0	4.76	47150
Regular B	975	80.1	4.39	46652
ASR A1	260	63.7	3.24	35750
ASR B1	610	67.1	---	32600
ASR B2	995	63	3.18	28100

Table 4. Reinforcement Steel Properties (Habibi et al., 2015)

Property	A_s (mm^2)	f_y (MPa)	f_u (MPa)	ε_{sh} (x10^{-3})	ε_u (x10^{-3})	E_s (MPa)
10M	100	430	638	8	150	182,000
20M	300	465	550	15	200	190,000

Table 5. Reinforcement Ratio (Habibi et al., 2015)

Specimen	$\rho_{h, web}$ (%)	$\rho_{v, web}$ (%)	$\rho_{h, flange}$ (%)	$\rho_{v, flange}$ (%)	$\rho_{z, flange}$ (%)
Regular A	0.80	0.77	067	2.10	0.44
ASR A1	0.80	0.77	0.67	2.10	0.44

Table 6. Tested ASR Expansion under Different Ages

	ASR A1	ASR B1	ASR B2
ASR expansion (%)	0.185	0.215	0.223
Age (days)	260	610	995

Benchmark Analysis with Post-testing Data

The benchmark analyses from 3D discrete model were compared with test results, and the results are shown in Figures 6 and 7 for the walls with regular and ASR concretes.

It is shown in Figure 6 that for regular concrete, the peak shear force in the test is 1180 KN, and the peak force from the 3D analysis is 1170 KN. The displacement at peak load is about 5.1 mm (as shown in red dots in the plots). As shown in Figure 7, for ASR concrete, the peak shear force in the test is 1355 KN, and the peak force from the FEA is 1255 KN. The displacement at peak load is about 5.2 mm (as shown in red dots in the plots).

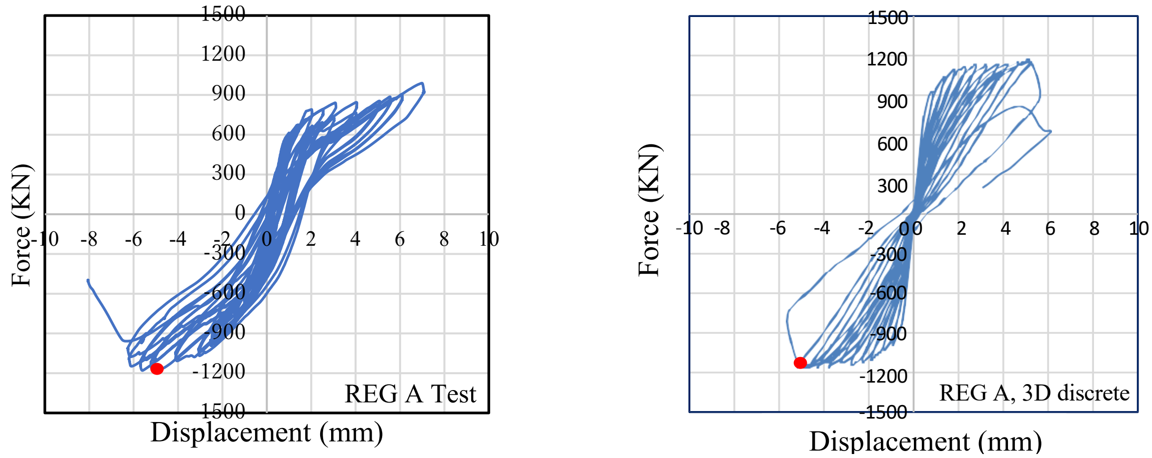

Figure 6. Comparison of Load-Displacement Curves between Test (left) [Habibi et al., 2015] and Analysis (right) for Regular Concrete

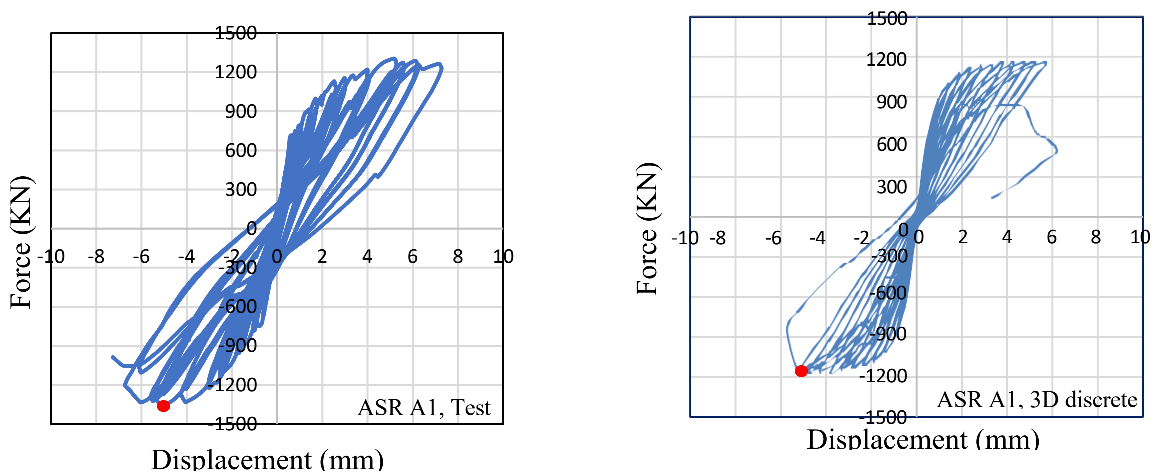

Figure 7. Comparison of Load-Displacement Curves between Test (left) [Habibi et al., 2015] and Analysis (right) for ASR Concrete (ASR 1 wall tested at 260 days of aging)

The comparison of the crack pattern and deflected shape at failure between the test and analysis is shown in Figure 8.

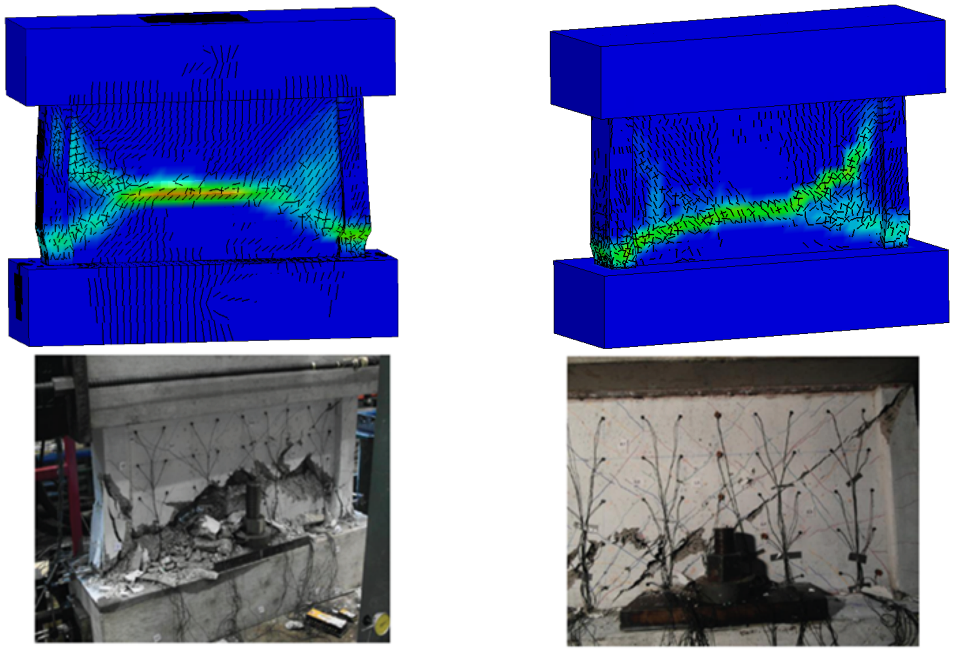

REG A ASR A1

Figure 8. Crack Pattern and Deflected Shape at the End of Test and Analysis for the Wall with Regular Concrete and the Wall with ASR Concrete Tested at 260 Days

Effect of Maximum Aggregate Size on ASR B1 Shear Wall

The 3D discrete model was used to study the effect of aggregate size on the ASR B1 shear wall load response and failure mode. The maximum aggregate sizes of 10 mm and 20mm were chosen for the sensitivity analysis for ASR B1 shear wall using 3D discrete model. The maximum aggregate size does not have significant effect on the peak cyclic load in the current analyses. The comparison of crack pattern and deflected shape between the analyses is shown in Figure 9. It is shown that the smaller aggregate size makes the ASR concrete failure in the earlier stage, since the concrete fracture energy and aggregate interlock are lower for smaller aggregate size, which can be seen clearly in cyclic load-displacement curves, shown in Figure 10. The results also shown that the failure mode changes with the changes in the aggregate size.

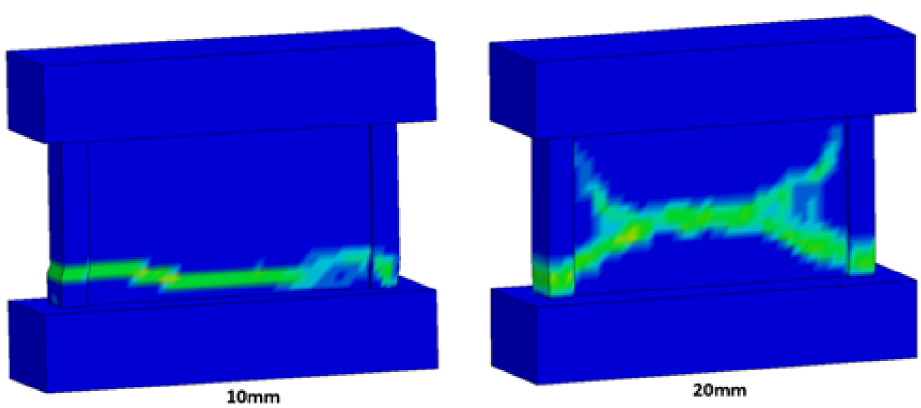

Figure 9. Failure Mode of ASR B1 Concrete Shear Wall with Different Aggregate Sizes

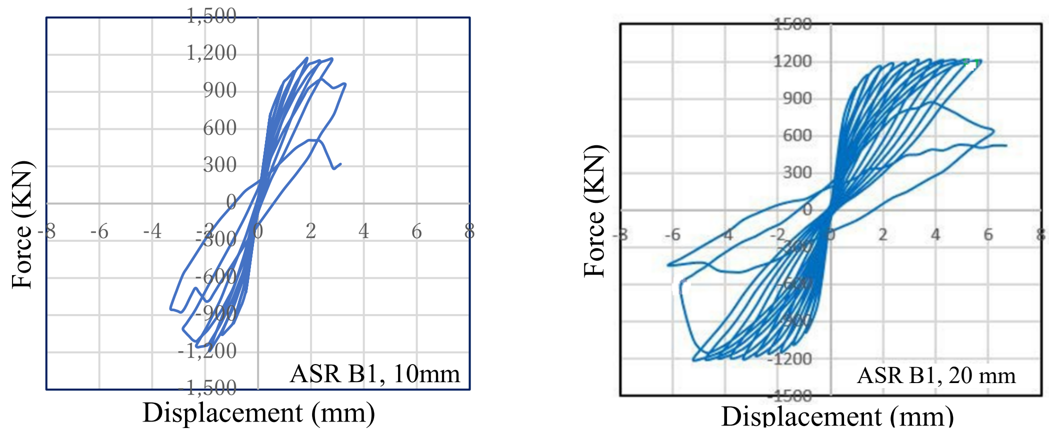

Figure 10. Effect of Aggregate Size on Cyclic Load vs. Displacement for ASR B1 Concrete Wall

Effect of ASR Expansion on ASR Concrete Capacity

To isolate the effect of the maximum unconfined ASR expansion on the concrete capacity, only the ASR expansion was changed (i.e., 0.3%, 0.4%), and all other input parameters were kept unchanged from the baseline modelling to study the effect of ASR expansion on the failure mode and peak load capacity for ASR B1 shear wall using 3D discrete model. The aggregate size is the 20mm baseline input. The final ASR expansions in this study do not have significant effect on the ASR concrete capacity, but the failure mode and ductility are affected, as shown in Figure 11.

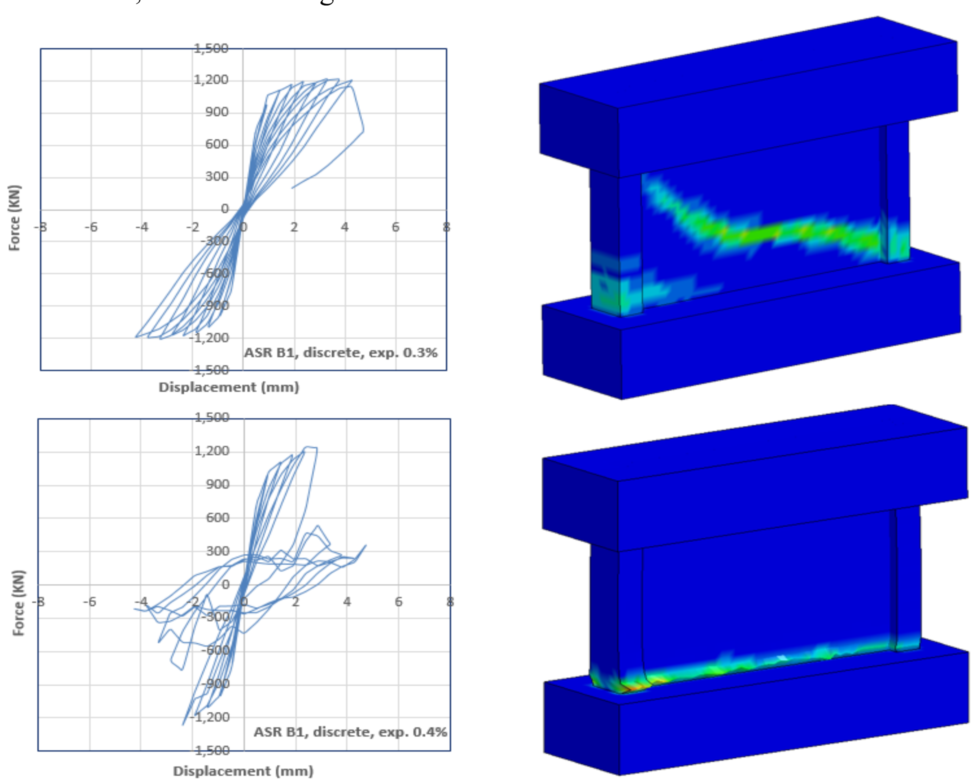

Figure 11. Response of ASR B1 wall for Different Maximum ASR Expansions and Calculated Crack Patterns and Deflected Shapes at the End of the Analysis (aggregate size: 20mm)

CONCLUSIONS

Benchmark analyses are performed for both regular concrete (240 days) and ASR concrete (260 days) and the calculated strength and ductility estimate the test results well. The regular concrete wall tested at 975 showed a small increase in strength as compared to the regular concrete wall tested at 240 days, and the wall failure was observed at about 8 mm displacement. A sensitivity study for the response of the wall with ASR concrete tested at 610 days was conducted, and it was found that for the wall with the ASR-affected concrete the analysis model indicates that the cyclic ductility reduces with increase in the maximum ASR expansion for expansion of 0.3% or greater. The peak cyclic load is not sensitive to the aggregate size for the walls with ASR concrete, but use of smaller aggregate size in the analysis leads to failure in fewer load cycles for the ASR-affected wall.

Disclaimer – This paper was prepared under the auspices of the U.S. Government. Neither the U.S. Government nor any agency thereof, nor any of their employees, makes any warranty, expressed or implied, or assumes any legal liability or responsibility for any third party's use, or the results of such use, of any information, apparatus, product, or process disclosed in this report, or represents that its use by such third party would not infringe privately owned rights. The views expressed in this paper are not necessarily those of the U.S. Nuclear Regulatory Commission.

REFERENCES

Habibi, F., Sheikh, S. A., Orbovic, N., Panesar, D. K., and Vecchio, F. J., "*Alkali Aggregate Reaction in Nuclear Concrete Structures: Part 1: Structural Wall Element Aspects*," Proceedings, *SMiRT23*, Manchester, U.K, August 10-14, 2015.

Vecchio, F.J. (2000). "*Disturbed Stress Field Model for Reinforced Concrete: Formulation*", *Journal of Structural Engineering*, 126(8), 1070-1077.

Vecchio, F.J., (1992). "*Finite Element Modelling of Concrete Expansion and Confinement*", *ASCE, Journal of Structural Engineering*, 118(9), 46-56.

Vecchio, F.J., and Collins, M.P. (1986). "*The Modified Compression Field Theory for Reinforced Concrete Elements Subjected to Shear*", *ACI Journal*, 83(2), 219-231.

Wong, P. S., Vecchio, F. J. and Trommels, H. (2002). "*VecTor2 and Formworks User's Manual*," Second Edition, University of Toronto, Toronto, Canada.

Jurcut, A. C., "*Modelling of Alkali-Aggregate Reaction Effects in Reinforced Concrete Structure*", thesis for the degree of Master of Applied Science, Civil Engineering, University of Toronto, 2015.